Terr. Atmos. Ocean. Sci., Vol. 25, No. 5, 719-726, October 2014 doi: 10.3319/TAO.2014.04.17.01(A)

NOTES AND CORRESPONDENCE

Barotropic Interactions Between Summertime Tropical Cyclones/Sub-Monthly Wave Patterns and Intraseasonal Oscillations over the Western North Pacific

Ken-Chung Ko[1,*] and Huang-Hsiung Hsu[2]

[1] *Department of Geography, National Kaohsiung Normal University, Kaohsiung, Taiwan*
[2] *Research Center for Environmental Changes, Academia Sinica, Taipei, Taiwan*

Received 29 December 2013, revised 17 March 2014, accepted 17 April 2014

ABSTRACT

This study used the barotropic kinetic energy conversion to record the active eddy-mean flow interaction between the TC/sub-monthly wave pattern (TSM) and the intraseasonal oscillation (ISO) in the western North Pacific (WNP). Overall, the TSM extracted (lost) kinetic energy from (to) the cyclonic (anticyclonic) circulation of the ISO, which is located in the South China Sea and the Philippine Sea, during the ISO westerly (easterly) phase. The phase change in barotropic energy conversion was due to the opposite background flow set up by the ISO. When the climatological-mean southwesterly was retained as part of the background flow in both ISO westerly and easterly phases as in previous studies, the ISO along with the low-frequency background flow always provided kinetic energy to the TSM regardless of the phase. The stronger (weaker) southwesterly in the ISO westerly (easterly) phase, the stronger (weaker) energy conversion to the TSM. Climatological mean flow exclusion showed an upscale feedback in the TSM to the ISO during the easterly phase. However, this feedback was weaker than the downscale conversion from the ISO to the TSM during the westerly phase.

Key words: Barotropic conversion, Intraseasonal oscillations, Submonthly wave, Tropical cyclones

Citation: Ko, K. C. and H. H. Hsu, 2014: Barotropic interactions between summertime tropical cyclones/sub-monthly wave patterns and intraseasonal oscillations over the western North Pacific. Terr. Atmos. Ocean. Sci., 25, 719-726, doi: 10.3319/TAO.2014.04.17.01(A)

1. INTRODUCTION

The western North Pacific (WNP) exhibits a wide range of multi-scale phenomena (hereafter KH06: Lau and Lau 1990; Liebmann et al. 1994; Ko and Hsu 2006; Hsu 2012). A crucial issue over the last decade has been the interaction between phenomena of different scales (e.g., hereafter KH09: Maloney and Dickinson 2003; Ko and Hsu 2009; hereafter KHC12: Maloney and Hartmann 2001; Chen and Sui 2010; Zhou and Li 2010; Ko et al. 2012). Studies have focused mostly on the intraseasonal oscillation (ISO) modulation effect on tropical cyclones (hereafter TCs) along with the sub-monthly or synoptic perturbations. A recent study by Hsu et al. (2011) found that the low frequency background flow always supplied energy to the synoptic eddies regardless of the ISO phases. Intraseasonal perturbations lost energy to synoptic eddies in the ISO active phase; whereas they gained energy from the synoptic eddies in the ISO suppressed phase.

The importance of the TC/sub-monthly wave pattern (TSM) has been reported by KH06 and KH09. Unlike the other bi-weekly (10 - 24 day) wave that tends to propagate westward from the Philippine Sea to the Indo-China Peninsula and the Bay of Bengal (Chen and Chen 1995; Chen et al. 2000), the TSM is a northwestward-propagating wave-like feature with TC embedded in the cyclonic circulation and the spectrum of this wave-like feature exhibits maxima around 7 - 30 days. KHC12 investigated a kinetic energy budget study of the TSM. The barotropic energy conversion from the background flow exhibited a maximum near the center of the TSM. Downscale energy conversion, preconditioned by the background flow, is observed in both the ISO westerly and easterly phases. No upscale conversion

* *Corresponding author*
E-mail: kko@nknu.edu.tw

from the TSM to ISO was found. However, because the background flow adopted in KHC12 included the long-term mean and perturbations with periods longer than intraseasonal time scales, this downscale energy conversion from the low-frequency perturbation might overshadow the possible upscale energy conversion from the TSM to ISO perturbations even if it did occur. The current study explored this possibility and investigated the barotropic energy conversion between the ISO and TSM perturbations by removing long-term mean and low-frequency perturbations from energy conversion calculation.

Figure 1 shows the stream function of the TSM and the corresponding ISO circulation anomalies at Day 0 (the peak time) in the westerly and easterly phases (KH09). As the TSM developed and moved northwestward in the WNP during the westerly phase, the corresponding ISO (30 - 80 day) was characterized by an east-west elongated cyclonic circulation. This was centered at approximately 20°N over the western Philippine Sea and the northern South China Sea (Fig. 1a). A well-organized TSM is under the influence of the ISO westerly anomaly between the equator and 20°N. By contrast, a loosely-organized wave pattern was observed under the influence of the anticyclonic circulation during the ISO easterly phase (Fig. 1b). The following question arises: how do the sub-monthly and intraseasonal perturbations interact kinematically in different ISO phases? For this study we computed the barotropic energy conversion for both ISO westerly and easterly phases to answer this question. Additionally, the major objective of this study, as an addition to previous studies, is to point out the possible upscale energy conversion from the TSM to ISO. This is an important point that was not explored in KHC12.

Section 2 describes the data and analysis procedures. The results are shown in section 3. Conclusions are presented in section 4.

2. DATA AND PROCEDURES

The data and cases selected for this study were the same as those used in KH09 and KHC12. The data were extracted from the European Centre for Medium-range Weather Forecast (ECMWF) re-analysis (ERA40, Uppala et al. 2005). The ERA40 contains 6-hourly (0000, 0600, 1200, and 1800 UTC) temperature, humidity, horizontal winds, pressure vertical velocity and geopotential on a 2.5° × 2.5° latitude-longitude grid. This study analyzed the data for July to September (JAS) over the 23-yr period from 1979 - 2001. A Butterworth band-passed filter (Kaylor 1977; Hamming 1989) was applied to extract the 7 - 30 day (sub-monthly) and 30 - 80 day (intraseasonal) fluctuations. A description of the case selection criteria is shown in the Appendix.

The perturbation kinetic energy (PKE) tendency equation for the TSM, following Lau and Lau (1992) is used to focus on the interaction between the perturbations and mean flow. The equation is rewritten as:

$$\frac{\partial \overline{K}}{\partial t} = -\overline{V_h'(V'\cdot\nabla)\overline{V}_h} - \overline{V}\cdot\nabla\overline{K} - \overline{V'\cdot\nabla K} - \frac{R}{P}\overline{\omega'T'} - \nabla\cdot(\overline{V'\Phi'}) + D \quad (1)$$

where the primes represent the 7 - 30 day filtered perturbations and the overbars stand for the 11-day period averages centered at the peak time for all westerly and easterly cases, respectively. The 11-day averaging was chosen to cover most of the selected TSM cases (with less overlapping), which fluctuated in varying periods from less than two-weeks to 20 days. Various numbers of averaging days (e.g., 20 days) were tested and the patterns were similar except for the strength. V is the three-dimensional velocity vector and V_h is the horizontal velocity vector, respectively. The PKE

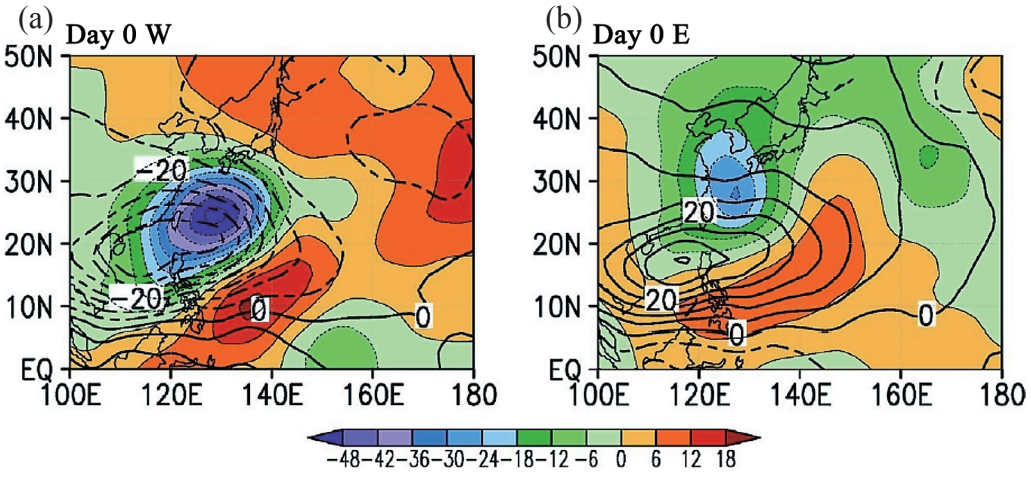

Fig. 1. Composites of 850 hPa sub-monthly (7 - 30 day) stream function (thin contours with shading) and the corresponding intraseasonal (30 - 80 day) stream function (thick contours) at Day 0 in the westerly (a) and easterly (b) phases. The interval was 3 (10^5 m^2 s^{-1}) for the sub-monthly parts and 10 (10^5 m^2 s^{-1}) for the other.

is represented by

$$K = \frac{1}{2}(u'^2 + v'^2) \tag{2}$$

where u' and v' are the 7 - 30 day filtered zonal and meridional wind components. The first term on the right in Eq. (1) represents the barotropic energy conversion (kp) that best describes the barotropic interaction between the perturbations and mean flow and it can be rewritten as:

$$kp = -\overline{u'^2}\frac{\partial\overline{u}}{\partial x} - \overline{u'v'}\frac{\partial\overline{u}}{\partial y} - \overline{u'v'}\frac{\partial\overline{v}}{\partial x} - \overline{v'^2}\frac{\partial\overline{v}}{\partial y} \tag{3}$$

The last two terms can be neglected (KHC12) and yield,

$$kp = -\overline{u'^2}\frac{\partial\overline{u}}{\partial x} - \overline{u'v'}\frac{\partial\overline{u}}{\partial y} \tag{4}$$

Let $u = u_l + u_i + u' + u_a$, where u_l, u_i, and u_a represent the low frequency (> 80 days), the ISO, and the high-frequency (< 7 day) components of the zonal wind. Due to the slowly varying nature of u_i compared with u', the resultant kp term yields,

$$kp = -\overline{u'^2}\frac{\partial u_l}{\partial x} - \overline{u'^2}\frac{\partial\overline{u_i}}{\partial x} - \overline{u'v'}\frac{\partial u_l}{\partial y} - \overline{u'v'}\frac{\partial\overline{u_i}}{\partial y} \tag{5}$$

The first and third terms on the right hand side represent the interaction between the low frequency and sub-monthly components. The barotropic interaction between the sub-monthly and ISO components (denoted as kp_{si}) can thus be written as:

$$kp_{si} = -\overline{u'^2}\frac{\partial\overline{u_i}}{\partial x} - \overline{u'v'}\frac{\partial\overline{u_i}}{\partial y} \tag{6}$$

The second and third terms of Eq. (1) stand for the mean advection and perturbation advection terms, respectively, and they are both small compared with the other terms (KHC12). The fourth term of Eq. (1) represents the baroclinic conversion term that maximizes at the upper levels (KHC12) and the fifth term of Eq. (1) is the generation term that does not show significant impact in the ISO and sub-monthly wave prevailing areas (KHC12). Dissipation is represented by the last term. Equation (1) describes the energetic budget terms between the mean state and perturbations and is different from that in Hsu et al. (2011) because they included terms that involve vertical fluxes and eddy-eddy interaction terms that are from the perturbation advection term. According to Mu and Zhang (2008), these terms are small (though they are non-zeroes) and the present study focuses on the interaction between the mean state and perturbations.

Unlike the KHC12 analysis which used climatological mean circulations of the westerly and easterly cases as the background flow, our analysis investigated the barotropic conversion term (denoted as kp_{si}), which represents the interaction between sub-monthly perturbations and ISO mean flow. The definitions of other terms render them unsuitable for examining the interaction between the TSM and ISO components (Hsu et al. 2011), and were thus ignored. This study focused on the kp_{si} term to delineate the interaction between the TSM and ISO.

3. RESULTS

The composite 7 - 30 and 30 - 80 day PKE maps in the westerly and easterly phases are shown in Fig. 2. The ISO PKE changed slowly over time and exhibited 2 maxima during the sub-monthly cycle. One of these maxima in the westerly phase was elongated and extended from 20°N, 135°E to southern Vietnam. The other maximum had a bull's-eye shape and was located over the East China Sea. These 2 PKE maxima were in agreement with the enhanced southwesterly flow and southeasterly flow in the southern and northeastern flanks of the ISO-westerly cyclonic circulation, respectively (Fig. 1). The sub-monthly PKE at Day -3 in the westerly phase exhibited a maximum centered near 20°N, 130°E; that is, near the northeastern corner of the southern ISO PKE maximum. The sub-monthly PKE maximum at the peak phase (Day 0) moved farther northwestward and expanded in spatial coverage while reaching peak amplitude. The sub-monthly PKE maximum weakened 3 days later (i.e., Day 3) when the sub-monthly cyclonic circulation moved quickly northeastward to the midlatitudes (KH09). During the same period the northeastern portion of the southern ISO maximum in the westerly phase also shrank a little from Day 0 to 3 (Figs. 2c and e). In the easterly phase, 2 ISO PKE maxima were also observed over similar regions but were weaker than their westerly counterparts. Although the TSM and ISO PKE maxima were weaker than that in the westerly phase, an eastward/northeastward expansion of the southern ISO PKE maximum was evident from Day -3 to 3 (Figs. 2b, d, and f).

We investigated the interaction between the TSM and ISO by examining the cross sections of the kp_{si} term averaged over 11 days, centered at the peak time (Day 0) of the sub-monthly cases for both ISO phases (Fig. 3). In order to illustrate the significance of the interaction a student t-test was performed to the kp_{si} term based on the population of the kp_{si} term at each time calculated in the same way as in Eq. (6) (with degree of freedom 40 and 24 for westerly and easterly phase). The longitudinal band (125° - 135°E) is chosen because it represents the overlapping zone between the TSM and ISO. Figure 3a shows a kp_{si} maximum centered near 15° - 20°N and this maximum area extended from

the surface to 400 hPa and peaked in the lower troposphere in the westerly phase. This area was also co-located with the PKE maxima of both ISO and TSM, suggesting that the supply of the PKE from the ISO to the TSM tended to sustain the TSM. Immediately north of the kp_{si} maximum around 28°N, a kp_{si} minimum (negative maximum) occurred, indicating that PKE energy flowed from the TSM to the ISO. However, it was too weak to be statistically significant. Because the negative kp_{si} term was considerably weaker and confined to a substantially smaller area, the net kp_{si} term below 400 hPa in this domain is positive overall. That is, kinetic energy was converted from the ISO to the TSM.

The situation differed in the ISO easterly phase (Fig. 3b). The amplitude of ISO PKE was roughly 2/3 of its counterpart

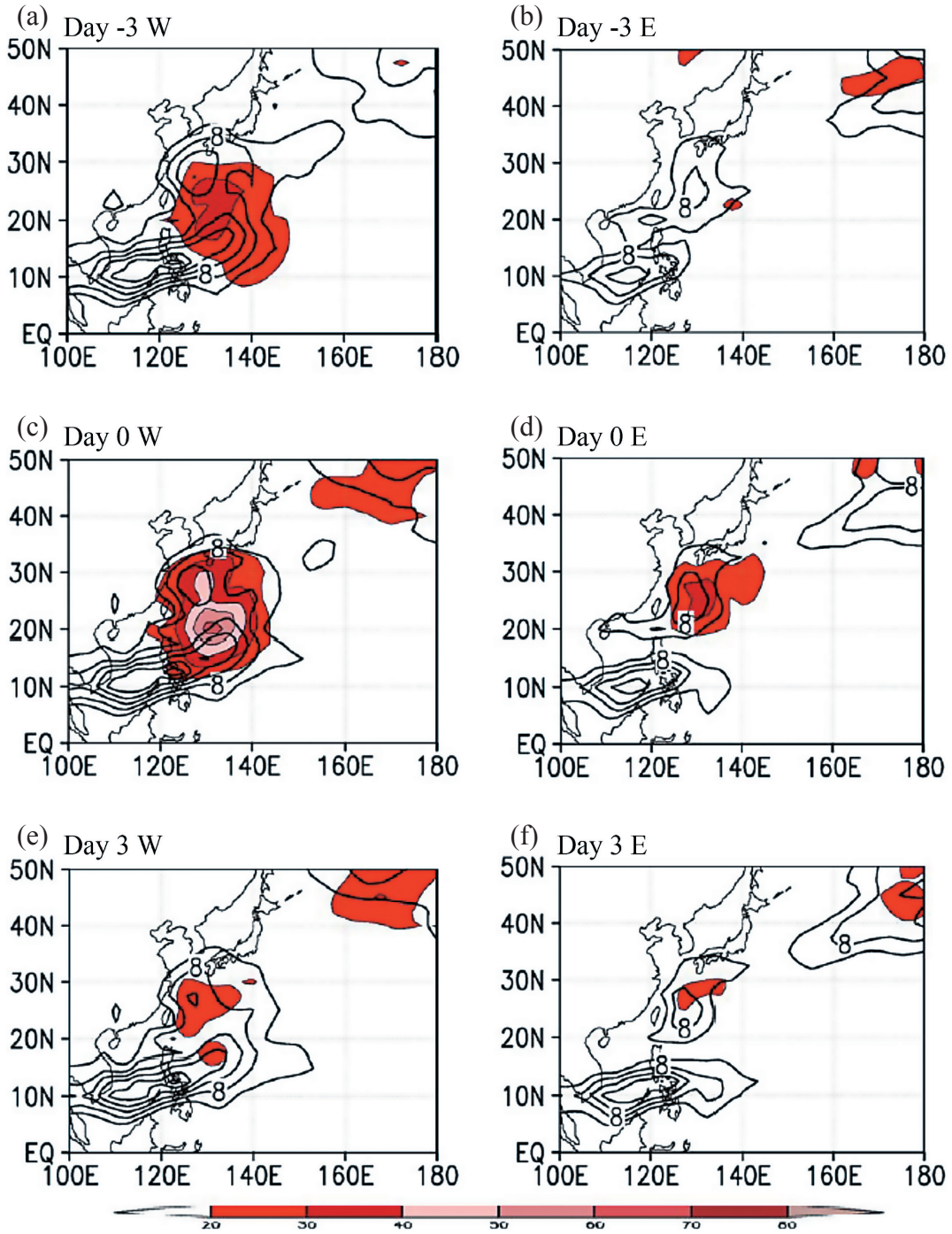

Fig. 2. Composites of 850 hPa sub-monthly (7 - 30 day) kinetic energy (thin contours with shading) and the corresponding intraseasonal (30 - 80 day) kinetic energy (thick contours) at Day -3, 0, and 3 in the westerly (a, c, and e) and easterly (b, d, and f) phases. The interval was 10 ($m^2 s^{-2}$) for the sub-monthly parts and 2 ($m^2 s^{-2}$) for the other.

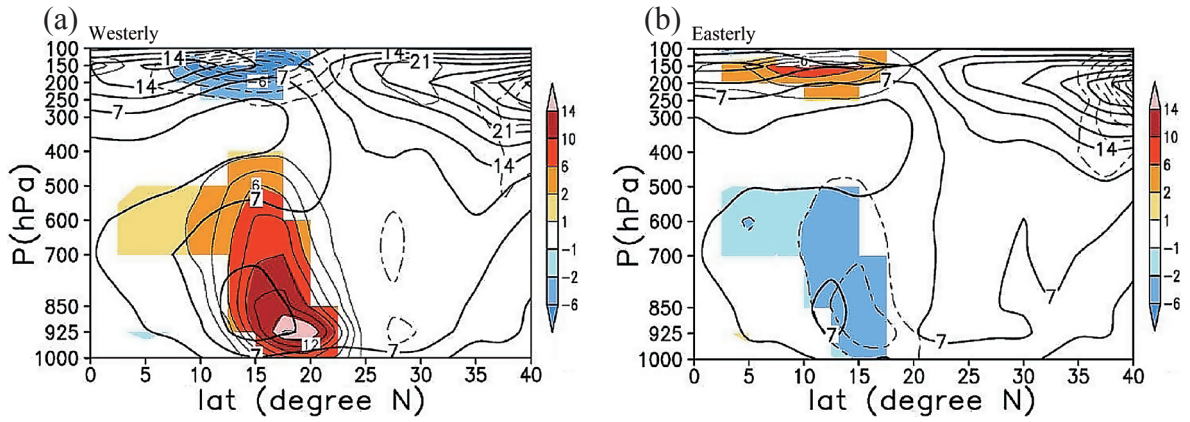

Fig. 3. Composite 11-day averaged cross sections (125° - 135°E) for the barotropic term (thin contours) between 7 - 30 and the 30 - 80 day PKE in the ISO westerly (a) and easterly (b) phases. The interval is 2 (10^{-5} m^2 s^{-3}). The areas exceeding the 95% confidence levels are shaded. Also shown are the 30 - 80 day PKE (thick contours and the interval was 3.5 m^2 s^{-2}).

in the westerly phase. The kp_{si} term was negative and located around 15°N, a region north of the ISO PKE maximum. The negative kp_{si} term was located to the south of maximum TSM PKE. This relative distribution suggests that the kinetic energy conversion supplied the kinetic energy from north (TSM PKE maximum) to south (ISO PKE maximum) and enhanced the ISO PKE (caused an eastward/northeastward expansion of the southern ISO PKE maximum from Day -3 to 3 as in Figs. 2b, d, and f) in the ISO easterly phase. While the upscale energy conversion was weak and relatively unimportant in the westerly phase (Fig. 3a) it was the main feature in the easterly phase (Fig. 3b). The contrasting results indicate the two-way interaction between the TSM and ISO.

The energy conversion accompanying the circulation at 850 hPa (a level close to the maximum PKE and kp_{si} term) was further examined to demonstrate the conversion between the TSM and ISO PKE. The results are shown in Fig. 4. The maximum zone of the positive kp_{si} term was evident northeast of the ISO PKE maximum zone in the ISO westerly phase (Fig. 4a). This spatial connection along with the intraseasonal flow pattern indicated that the ISO westerly flow pattern (Fig. 4a) was characterized by a strong cyclonic circulation; this would bring strong southwesterly flow to this area and supply energy to the TSM PKE (KH09). By contrast, the anticyclonic circulation in the ISO easterly phase (Fig. 4b) drained kinetic energy from the TSM to the ISO.

Kinetic energy peaked in the lower troposphere and the kp_{si} term was dominated by $-\overline{u'^2}\frac{\partial \overline{u_i}}{\partial x}$ and $-\overline{u'v'}\frac{\partial \overline{u_i}}{\partial y}$. These two terms were further examined as shown in Figs. 4c - f. The 30 - 80 day zonal wind in the westerly phase (Figs. 4c and e) was characterized by a slight eastnortheast - westsouthwest tilted maximum zone centered at 10°N near the central South China Sea, with a minimum zone from southeastern China to the East China Sea. The $\overline{u'^2}$ maximum was located over the northeastern corner of the ISO zonal wind maximum zone where $\frac{\partial \overline{u_i}}{\partial x}$ was negative southeast of the $\overline{u'^2}$ maximum and resulted in a $-\overline{u'^2}\frac{\partial \overline{u_i}}{\partial x}$ maximum. A secondary $\overline{u'^2}$ maximum was located near the eastern portion of the ISO zonal wind minimum where $\frac{\partial \overline{u_i}}{\partial x}$ was positive indicating that a weak negative $-\overline{u'^2}\frac{\partial \overline{u_i}}{\partial x}$ area was located north of the mentioned $-\overline{u'^2}\frac{\partial \overline{u_i}}{\partial x}$ maximum. The distribution of $\overline{u'v'}$ revealed a maximum area over the northeastern corner of the ISO zonal wind maximum zone where $\frac{\partial \overline{u_i}}{\partial y}$ was negative resulting in a $-\overline{u'v'}\frac{\partial \overline{u_i}}{\partial y}$ maximum. These 2 maxima formed the resultant kp_{si} maximum in the westerly phase, as shown in Fig. 4a.

The $\overline{u'^2}$ and $\overline{u'v'}$ distribution in the easterly phase (Figs. 4d and f) was similar to that in the westerly phase but showed a far weaker amplitude. The ISO zonal wind pattern was north-south reversed due to the ISO anticyclonic circulation as seen in Fig. 1. Although weaker $\overline{u'^2}$ and $\overline{u'v'}$ maxima continued, proximal to similar locations as in the westerly phase, the kp_{si} term was mainly negative along the northern edge of the ISO PKE. These results indicated that the TSM mainly extracted kinetic energy from the ISO flow in the westerly phase but lost kinetic energy to the ISO flow during the easterly phase. The upscale versus downscale nature of energy conversion was determined by the background flow.

4. CONCLUSIONS

This study investigated the interaction between the TSM and ISO in the WNP. The kp_{si} term of the TSM PKE equation was computed using the sub-monthly component with the perturbations and ISO component as the background flow. Our results showed that, in the westerly phase, a kp_{si} maximum area existed along 15° - 20°N, indicating that the PKE is supplied from the ISO to the TSM. In the easterly phase, however, the area along 15° - 20°N was occupied by a kp_{si} negative maximum. This observation showed that the TSM supplied PKE to the ISO and caused an eastward/northeastward expansion of the southern ISO PKE maximum at approximately 15° - 20°N.

Overall, positive kp_{si} dominated in the westerly phase, while negative kp_{si} dominated in the easterly phase. The kinetic energy flow directions between these 2 oscillating phenomena are shown in the schematic diagrams in Fig. 5. The area-averaged (boxes as in Fig. 4) kp_{si} as in KHC12 showed energy flow from the climatological mean flow to

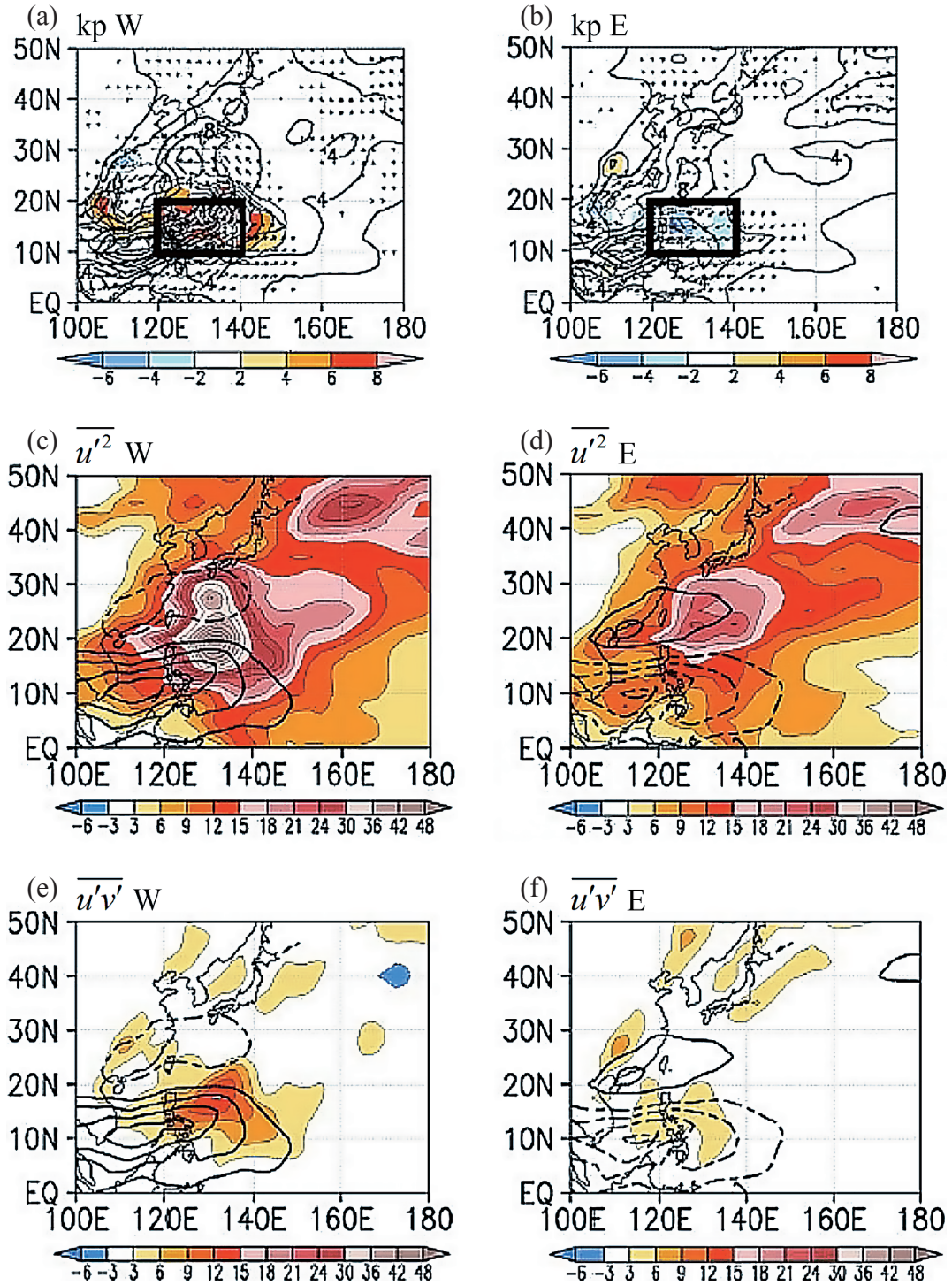

Fig. 4. Composites of 11-day averaged 850 hPa barotropic conversion (thin contours) between the sub-monthly (7 - 30 day) and the corresponding intraseasonal (30 - 80 day) fields in the (a) westerly and (b) easterly phases. The areas exceeding the 95% confidence levels are shaded. Also shown are the 30 - 80 day PKE (thick contours) and wind vectors. The interval is 2(10^{-5} m^2 s^{-3}) for the barotropic conversion and is 2 (m^2 s^{-2}) for the 30 - 80 day PKE. The boxes in (a) and (b) are for area-averages of barotropic terms. $\overline{u'^2}$ and $\overline{u'v'}$ are shaded in the westerly [(c) and (e)] and easterly [(d) and (f)] phases and also shown in (c), (d), (e), and f are the corresponding 30 - 80 day zonal wind $\overline{u_i}$ (thick contour) fields. The unit for $\overline{u'^2}$ and $\overline{u'v'}$ is m^2 s^{-2} and is ms^{-1} for $\overline{u_i}$. The contour interval for $\overline{u'^2}$ and $\overline{u'v'}$ is 3 and is 1 for $\overline{u_i}$.

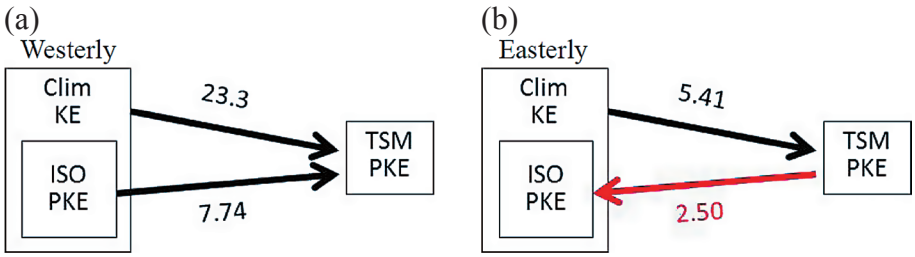

Fig. 5. Schematic diagrams for the barotropic conversion (10^{-5} m^2 s^{-3}) between the climatological mean flow/intraseasonal flow and the sub-monthly fields for the westerly (a) and easterly (b) phases. The numbers indicate the area-averaged (boxes as in Fig. 4) barotropic terms. The red arrow represents a negative value which means the energy flows from the TSM to ISO.

the TSM in both phases, and the kp_{si} exhibited much greater energy flow in the westerly (23.3×10^{-5} m^2 s^{-3}) than in the easterly (5.41×10^{-5} m^2 s^{-3}) phase using the ISO westerly and easterly climatological mean flow patterns. However, the present study removed the climatological component and used the ISO flow as in Eqs. (5) and (6). Our findings were dissimilar to those obtained by KHC12. The area-averaged kp_{si} was 7.74×10^{-5} m^2 s^{-3} in the westerly phase and -2.50×10^{-5} m^2 s^{-3} in the easterly phase, indicating that altering the background flow to the 30 - 80 day filtered data resulted in almost opposite kp_{si} patterns for the ISO westerly versus easterly phases. Downscale energy conversion from the ISO to the TSM occurred in the ISO westerly phase, whereas upscale energy conversion was observed in the ISO easterly phase. The aforementioned energy flow also indicates that the TSM during the ISO easterly phase should have less energy, weaker intensity and shorter lifespan than its counterpart during the westerly phase. The TSM structure as in KH09 supports this point because the TSM is better organized in the westerly phase.

Acknowledgments We thank the two Anonymous Reviewers for their comments that improved the quality of this manuscript. This study was supported by the National Science Council, Taiwan under Grant NSC 102-2111-M-017-001 issued to Ken-Chung Ko and Grant NSC 100-2119-M-001-029-MY5 issued to Huang-Hsiung Hsu.

REFERENCES

Chen, G. and C. H. Sui, 2010: Characteristics and origin of quasi-biweekly oscillation over the western North Pacific during boreal summer. *J. Geophys. Res.*, **115**, D14113, doi: 10.1029/2009JD013389. [Link]

Chen, T. C. and J. M. Chen, 1995: An observational study of the South China Sea monsoon during the 1979 summer: Onset and life cycle. *Mon. Weather Rev.*, **123**, 2295-2318, doi: 10.1175/1520-0493(1995)123<2295:AOSOTS>2.0.CO;2. [Link]

Chen, T. C., M. C. Yen, and S. P. Weng, 2000: Interaction between the summer monsoons in East Asia and the South China Sea: Intraseasonal monsoon modes. *J. Atmos. Sci.*, **57** 1373-1392, doi: 10.1175/1520-0469(2000)057<1373:IBTSMI>2.0.CO;2. [Link]

Hamming, R. W., 1989: Digital Filters, Dover Publications, 284 pp.

Hsu, H. H., 2012: Intraseasonal variability of the atmosphere-ocean-climate system: East Asian monsoon. In: Lau, W. K. M. and D. E. Waliser (Eds.), Intraseasonal Variability in the Atmosphere-Ocean Climate System, Springer Praxis Books, Springer Berlin Heidelberg, UK, Chichester, 73-110, doi: 10.1007/978-3-642-13914-7_3. [Link]

Hsu, P., T. Li, and C. H. Tsou, 2011: Interactions between boreal summer intraseasonal oscillations and synoptic-scale disturbances over the western North Pacific. Part I: Energetics diagnosis. *J. Climate*, **24**, 927-941, doi: 10.1175/2010JCLI3833.1. [Link]

Kaylor, R. E., 1977: Filtering and decimation of digital time series. Tech. Note BN 850, Institute of Physical Science Technology, University of Maryland, College Park, 42 pp.

Ko, K. C. and H. H. Hsu, 2006: Sub-monthly circulation features associated with tropical cyclone tracks over the East Asian monsoon area during July-August season. *J. Meteorol. Soc. Jpn.*, **84**, 871-889, doi: 10.2151/jmsj.84.871. [Link]

Ko, K. C. and H. H. Hsu, 2009: ISO Modulation on the sub-monthly wave pattern and recurving tropical cyclones in the tropical western north Pacific. *J. Climate*, **22**, 582-599, doi: 10.1175/2008JCLI2282.1. [Link]

Ko, K. C., H. H. Hsu , and C. Chou, 2012: Propagation and maintenance mechanism of the TC/submonthly wave pattern and TC feedback in the western North Pacific. *J. Climate*, **25**, 8591-8610, doi: 10.1175/JCLI-D-11-00643.1. [Link]

Lau, K. H. and N. C. Lau, 1990: Observed structure and propagation characteristics of tropical summertime synoptic scale disturbances. *Mon. Weather Rev.*, **118**, 1888-1913, doi: 10.1175/1520-0493(1990)118<1888:OSAPCO>2.0.CO;2. [Link]

Lau, K. H. and N. C. Lau , 1992: The energetics and

propagation dynamics of tropical summertime synoptic-scale disturbances. *Mon. Weather Rev.*, **120**, 2523-2539, doi: 10.1175/1520-0493(1992)120<2523:TEAPDO>2.0.CO;2. [Link]

Liebmann, B., H. H. Hendon, and J. D. Glick, 1994: The relationship between tropical cyclones of the western Pacific and Indian Oceans and the Madden-Julian oscillation. *J. Meteorol. Soc. Jpn.*, **72**, 401-412.

Maloney, E. D. and M. J. Dickinson, 2003: The intraseasonal oscillation and the energetics of summertime tropical western North Pacific synoptic-scale disturbances. *J. Atmos. Sci.*, **60**, 2153-2168, doi: 10.1175/1520-0469-(2003)060<2153:TIOATE>2.0.CO;2. [Link]

Maloney, E. D. and D. L. Hartmann, 2001: The Madden-Julian oscillation, barotropic dynamics, and north Pacific tropical cyclone formation. Part I: Observations. *J. Atmos. Sci.*, **58**, 2545-2558, doi: 10.1175/1520-0469-(2001)058<2545:TMJOBD>2.0.CO;2. [Link]

Mu, M. and G. J. Zhang, 2008: Energetics of Madden Julian oscillations in the NCAR CAM3: A composite view. *J. Geophys. Res.*, **113**, D05108, doi: 10.1029/2007JD008700. [Link]

Uppala, S. M., P. W. Kållberg, A. J. Simmons, U. Andrae, V. Da Costa Bechtold, M. Fiorino, J. K. Gibson, J. Haseler, A. Hernandez, G. A. Kelly, X. Li, K. Onogi, S. Saarinen, N. Sokka, R. P. Allan, E. Andersson, K. Arpe, M. A. Balmaseda, A. C. M. Beljaars, L. van de Berg, J. Bidlot, N. Bormann, S. Caires, F. Chevallier, A. Dethof, M. Dragosavac, M. Fisher, M. Fuentes, S. Hagemann, E. Hólm, B. J. Hoskins, L. Isaksen, P. A. E. M. Janssen, R. Jenne, A. P. Mcnally, J. F. Mahfouf, J. J. Morcrette, N. A. Rayner, R. W. Saunders, P. Simon, A. Sterl, K. E. Trenberth, A. Untch, D. Vasiljevic, P. Viterbo, and J. Woollen, 2005: The ERA-40 re-analysis. *Q. J. R. Meteorol. Soc.*, **131**, 2961-3012, doi: 10.1256/qj.04.176. [Link]

Zhou, C. and T. Li, 2010: Upscale feedback of tropical synoptic variability to intraseasonal oscillations through the nonlinear rectification of the surface latent heat flux. *J. Climate*, **23**, 5738-5754, doi: 10.1175/2010JCLI3468.1. [Link]

APPENDIX

The sub-monthly cases were selected based on the 7 - 30 day filtered time series of 850-hPa wind speed averaged over the base region between Taiwan and Japan (20° - 35°N, 125° - 140°E) where a variance in maximum wind speed existed. The sub-monthly cases were selected when the positive anomalous maxima were greater than 1 ms^{-1}, which was equivalent to 0.75 standard deviation. A tropical cyclone (TC)/sub-monthly case was further selected when at least a TC appeared in the base region (with a 1.5° latitude-longitude buffer zone just outside the edge) between Day -1 and Day +1 of a selected sub-monthly case. The TC/sub-monthly cases were further classified into two categories: ISO westerly and easterly phases. A TC/sub-monthly case was classified as a case in the westerly (easterly) phase if the anomalous 30 - 80 filtered zonal wind averaged over the ISO base region (5° - 15°N, 100° - 125°E), where the maximum variance in the intraseasonal zonal wind was located, at the occurrence time the sub-monthly case was greater than 1.5 ms^{-1} (less than -1.5 ms^{-1}). The ±1.5 ms^{-1} thresholds were approximately ±0.5 standard deviation of the 30- to 80-day filtered zonal wind time series. The resultant number of sub-monthly cases is 40 for the ISO westerly cases and 24 for the ISO easterly cases.